Supplementary Materials

Identifying determinants of γ' phase coarsening behavior in Co/CoNi-based superalloys with explainable artificial intelligence (XAI)

Linlin Sun[1,2], Qingshuang Ma[1,2], Jingwen Zhang[3], Liming Yu[3], Jie Xiong[4,*], Huijun Li[5], Qiuzhi Gao[1,2,*]

[1]School of Materials Science and Engineering, Northeastern University, Shenyang 110819, Liaoning, China.
[2]School of Resources and Materials, Northeastern University at Qinhuangdao, Qinhuangdao 066004, Hebei, China.
[3]School of Materials Science and Engineering, Tianjin University, Tianjin 300354, China.
[4]Materials Genome Institute, Shanghai University, Shanghai 200444, China.
[5]Faculty of Engineering and Information Sciences, University of Wollongong, Wollongong 2522, Australia.

***Correspondence to:** Dr. Jie Xiong, Materials Genome Institute, Shanghai University, 333 Nanchen Road, Shanghai 200444, China. E-mail: xiongjie@shu.edu.cn; Prof. Qiuzhi Gao, School of Materials Science and Engineering, Northeastern University, No.11, Lane 3, Wenhua Road, Shenyang 110819, Liaoning, China. E-mail: neuqgao@163.com

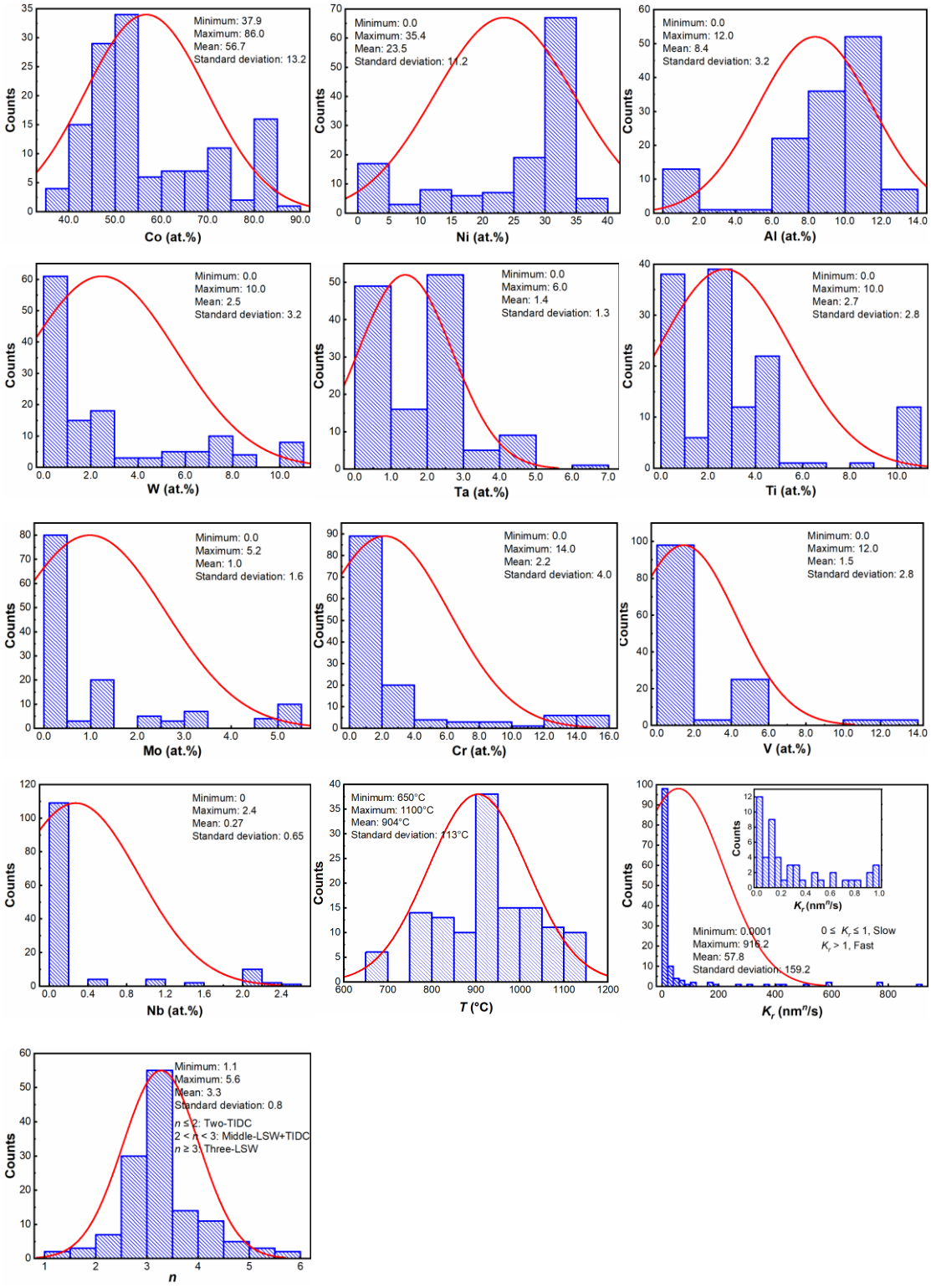

Supplementary Figure 1. Statistical distributions of element compositions, process parameter, n, and K_r in the investigated experimental datasets.

Supplementary Figure 2A shows a confusion matrix for the XGBC model using four SBS-selected CP features with cross-validation. In a confusion matrix, all samples can be categorized as true positive (TP), true negative (TN), false positive (FP), and false negative (FN), respectively. The precision and recall are defined by Supplementary Equation (1) and (2), respectively. Generally, there exists a precision-recall trade-off in classification, where an ML model often reduces recall with improving precision. The F_1 score, defined by Supplementary Equation (3), is the harmonic mean of precision and recall. The XGBC model yields the F1 scores of 0.900 and 0.939 for the Slow and Fast coarsening categories, respectively. Supplementary Figure 2B presents the receiver operating characteristic (ROC) curve for the Slow coarsening classification, plotting the true positive rate (TPR, equal to recall) against the false positive rate [FPR, see Supplementary Equation (4)]. The area under the ROC curve (AUC) is 0.908, indicating outstanding classification performance of the XGBC model[1].

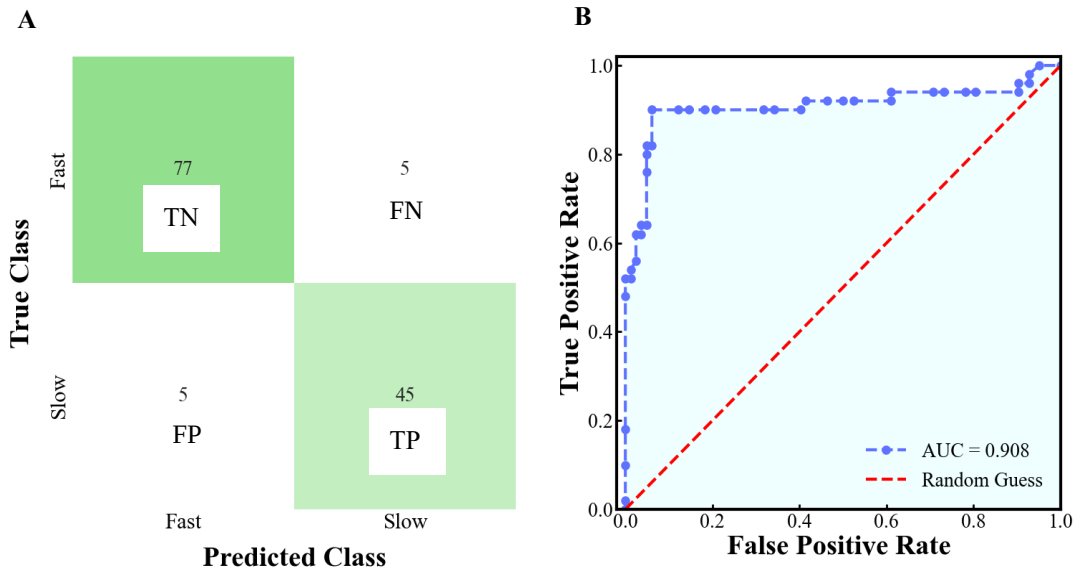

Supplementary Figure 2. The performance of XGBC model using four SBS-selected CP features with cross-validation. (A) the confusion matrix; (B) ROC curve with AUC for Slow coarsening category.

$$precision = \frac{TP}{TP + FP} \tag{S1}$$

$$recall = \frac{TP}{TP + FN} \tag{S2}$$

$$F_1 score = 2 \cdot \frac{precision \cdot recall}{precision + recall} \tag{S3}$$

$$FPR = \frac{FP}{FP + TN} \tag{S4}$$

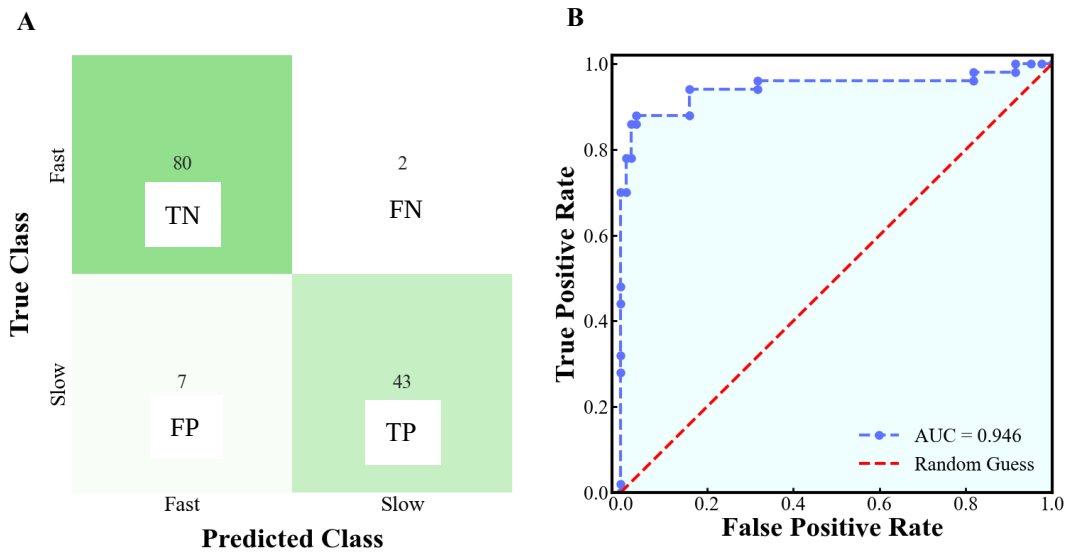

Supplementary Figure 3. The performance of XGBC model using seven SBS-selected CPAE features with cross-validation. (A) the confusion matrix; (B) ROC curve with AUC for Slow coarsening category.

Data Sources:

In this work, our methodology was applied on the $L1_2$-strengthened Co/CoNi-base superalloys data, which were collected from the relevant references[2-33], as detailed below:

[1] Hosmer D.W.; Lemeshow S.; Sturdivant R.X. *Applied logistic regression*, 3rd ed.; John Wiley & Sons, 2013. DOI: 10.1002/9781118548387

[2] Meher S.; Nag S.; Tiley J.; Goel A.; Banerjee R. Coarsening kinetics of γ′ precipitates in cobalt-base alloys. *Acta Mater.* **2013**, *61*, 4266-4276. DOI: 10.1016/j.actamat.2013.03.052

[3] Sauza D.J.; Bocchini P.J.; Dunand D.C.; Seidman D.N. Influence of ruthenium on microstructural evolution in a model CoAlW superalloy. *Acta Mater.* **2016**, *117*, 135-145. DOI: 10.1016/j.actamat.2016.07.014

[4] Vorontsov V.A.; Barnard J.S.; Rahman K.M.; Yan H.Y.; Midgley P.A.; Dye D. Coarsening behaviour and interfacial structure of γ′ precipitates in Co-Al-W based superalloys. *Acta Mater.* **2016**, *120*, 14-23. DOI: 10.1016/j.actamat.2016.08.023

[5] Bocchinia P.J.; Sudbrack C.K.; Noebe R.D.; Dunand D.C.; Seidman D.N. Effects of titanium substitutions for aluminum and tungsten in Co-10Ni-9Al-9W (at%) superalloys. *Mater. Sci. Eng., A* **2017**, *705*, 122-132. DOI:

10.1016/j.msea.2017.08.034
[6] Che C.; Yang S.; Wei M.; et al. Microstructure, hardness and interfacial energy in Co-9Al-10W-xNi (x=15, 25, 35 at.%) alloys during aging. *J. Min. Metall. Sect. B-Metall.* **2017**, *53*, 303-308. DOI: 10.2298/jmmb170531021c
[7] Zhou H.J.; Xue F.; Chang H.; Feng Q. Effect of Mo on microstructural characteristics and coarsening kinetics of γ′ precipitates in Co-Al-W-Ta-Ti alloys. *J. Mater. Sci. Technol.* **2018**, *34*, 799-805. DOI: 10.1016/j.jmst.2017.04.012
[8] Azzam A.; Philippe T.; Hauet A.; et al. Kinetics pathway of precipitation in model Co-Al-W superalloy. *Acta Mater.* **2018**, *145*, 377-387. DOI: 10.1016/j.actamat.2017.12.032
[9] Lass E.A.; Sauza D.J.; Dunand D.C.; Seidman D.N. Multicomponent γ′-strengthened Co-based superalloys with increased solvus temperatures and reduced mass densities. *Acta Mater.* **2018**, *147*, 284-295. DOI: 10.1016/j.actamat.2018.01.034
[10] Chen Y.C.; Wang C.P.; Ruan J.J.; et al. High-strength Co-Al-V-base superalloys strengthened by γ′-Co_3(Al,V) with high solvus temperature. *Acta Mater.* **2019**, *170*, 62-74. DOI: 10.1016/j.actamat.2019.03.013
[11] Sauza D.J.; Dunand D.C.; Noebe R.D.; Seidman D.N. γ′-($L1_2$) precipitate evolution during isothermal aging of a Co-Al-W-Ni superalloy. *Acta Mater.* **2019**, *164*, 654-662. DOI: 10.1016/j.actamat.2018.11.014
[12] Pandey P.; Kashyap S.; Palanisamy D.; Sharma A.; Chattopadhyay K. On the high temperature coarsening kinetics of γ′ precipitates in a high strength $Co_{37.6}Ni_{35.4}Al_{9.9}Mo_{4.9}Cr_{5.9}Ta_{2.8}Ti_{3.5}$ fcc-based high entropy alloy. *Acta Mater.* **2019**, *177*, 82-95. DOI: 10.1016/j.actamat.2019.07.011
[13] Qu S.S.; Li Y.J.; Wang C.P.; et al. Coarsening behavior of γ′ precipitates and compression deformation mechanism of a novel Co–V–Ta–Ti superalloy. *Mater. Sci. Eng., A* **2020**, *787*, 139455. DOI: 10.1016/j.msea.2020.139455
[14] Li C.; Chung D.W.; Dunand D.C.; Seidman D.N. Microstructural stability and mechanical behavior of a Co–20Ni–7Al–7W–4Ti at.% superalloy. *J. Alloys Compd.* **2020**, *848*, 156378. DOI: 10.1016/j.jallcom.2020.156378
[15] Chen Y.C.; Wang C.P.; Ruan J.J.; et al. Development of low-density γ/γ′ Co-Al-Ta-based superalloys with high solvus temperature. *Acta Mater.* **2020**, *188*, 652-664. DOI: 10.1016/j.actamat.2020.02.049
[16] Baler N.; Pandey P.; Palanisamy D.; Makineni S.K.; Phanikumar G.; Chattopadhyay K. On the effect of W addition on microstructural evolution and γ′

precipitate coarsening in a Co–30Ni–10Al–5Mo–2Ta–2Ti alloy. *Materialia* **2020**, *10*, 100632. DOI: 10.1016/j.mtla.2020.100632

[17] Singh M.P.; Makineni S.K.; Chattopadhyay K. Achieving lower mass density with high strength in Nb stabilised γ/γ′ Co–Al–Mo–Nb base superalloy by the replacement of Mo with V. *Mater. Sci. Eng., A* **2020**, *794*, 139826. DOI: 10.1016/j.msea.2020.139826

[18] Gao Q.Z.; Jiang Y.J.; Liu Z.Y.; et al. Effects of alloying elements on microstructure and mechanical properties of Co–Ni–Al–Ti superalloy. *Mater. Sci. Eng., A* **2020**, *779*, 139139. DOI: 10.1016/j.msea.2020.139139

[19] Zhuang X.L.; Antonov S.; Li L.F.; Feng Q. Effect of alloying elements on the coarsening rate of γ′ precipitates in multi-component CoNi-based superalloys with high Cr content. *Scr. Mater.* **2021**, *202*, 114004. DOI: 10.1016/j.scriptamat.2021.114004

[20] Qu S.S.; Li Y.J.; Tong M.; Wang C.P.; Yang Y.S. Effects of 1 at.% Ta substitution for 1 at.% W on the coarsening kinetics and deformation behavior of γ′-strengthened CoNi-base superalloys. *Mater. Sci. Eng., A* **2021**, *823*, 141776. DOI: 10.1016/j.msea.2021.141776

[21] Pandey P.; Shankar Prasad A.; Baler N.; Chattopadhyay K. On the effect of Ti addition on microstructural evolution, precipitate coarsening kinetics and mechanical properties in a Co–30Ni–10Al–5Mo–2Nb alloy. *Materialia* **2021**, *16*, 101072. DOI: 10.1016/j.mtla.2021.101072

[22] Pandey P.; Mazumder N.; Singh M.P.; et al. Design of low mass density γ/γ′ CoNi-based superalloys with promising high-temperature mechanical properties. *Phys. Rev. Mater.* **2021**, *5*, 093601. DOI: 10.1103/PhysRevMaterials.5.093601

[23] Mukhopadhyay S.; Pandey P.; Baler N.; Biswas K.; Makineni S.K.; Chattopadhyay K. The role of Ti addition on the evolution and stability of γ/γ′ microstructure in a Co-30Ni-10Al-5Mo-2Ta alloy. *Acta Mater.* **2021**, *208*, 116736. DOI: 10.1016/j.actamat.2021.116736

[24] Zhang X.M.; Shang H.; Gao Q.Z.; et al. Coarsening evolution of γ′ phase and failure mechanism of Co-Ni-Al-Ti-based superalloys during isothermal aging. *Front. Mater.* **2022**, *9*, 863305. DOI: 10.3389/fmats.2022.863305

[25] Liu X.J.; Cai W.S.; Chen Z.F.; et al. Effects of alloying additions on the microstructure, lattice misfit, and solvus temperature of a novel Co–Ni-based superalloy. *Intermetallics* **2022**, *141*, 107431. DOI: 10.1016/j.intermet.2021.107431

[26] Liu P.; Huang H.Y.; Jiang X.; et al. Evolution analysis of γ′ precipitate coarsening in Co-based superalloys using kinetic theory and machine learning. *Acta Mater.* **2022**, *235*, 118101. DOI: 10.1016/j.actamat.2022.118101

[27] Wang C.P.; Le J.P.; Chen K.Y.; et al. A novel Co-Ni-Ti-V-based superalloy exhibiting low density and high strength. *Mater. Sci. Eng., A* **2023**, *885*, 145633. DOI: 10.1016/j.msea.2023.145633

[28] Pandey P.; Pantawane M.V.; Baler N.; Ravi R.; Makineni S.K.; Chattopadhyay K. Effect of Cr addition on the γ′ strengthened CoNiCrAlMo compositionally complex alloy. *Mater. Sci. Technol.* **2023**, *39*, 347-361. DOI: 10.1080/02670836.2022.2114615

[29] Zhuang X.L.; Antonov S.; Li L.F.; Feng Q. γ′-Strengthened Multicomponent CoNi-Based Wrought Superalloys With Improved Comprehensive Properties. *Metall. Mater. Trans. A* **2023**, *54*, 1671-1682. DOI: 10.1007/s11661-023-06959-4

[30] Wang C.P.; Chen Y.H.; Zhuo H.J.; et al. Development of Co-Ni-Al-V-Ta-Cr-based superalloys with high-temperature strength and excellent oxidation resistance. *J. Mater. Res. Technol.* **2023**, *27*, 8143–8150. DOI: 10.1016/j.jmrt.2023.11.217

[31] Li J.L.; Zhang J.Q.; Li Z.; et al. Effect of Ti/Nb/Ta addition on the γ/γ′ coherent microstructure in low-density and high-strength Co-Al-W-Mo-based superalloys. *J. Mater. Sci. Technol.* **2024**, *186*, 174-187. DOI: 10.1016/j.jmst.2023.11.021

[32] Zhang X.R.; Zou M.; Lu S.; Li L.F.; Zhuang X.L.; Feng Q. A novel high-Cr CoNi-based superalloy with superior high-temperature microstructural stability, oxidation resistance and mechanical properties. *Int. J. Miner., Metall. Mater.* **2024**, *31*, 1373-1381. DOI: 10.1007/s12613-024-2843-6

[33] Le J.P.; Zhang J.B.; Zhang Y.P.; et al. Study of the experimental phase diagram and $L1_2$ Phase stability in the Co-Ni-Ti-V system. *SSRN* **2024**, Available online: https://ssrn.com/abstract=4681604 or http://dx.doi.org/10.2139/ssrn.4681604